OPTIMIZATION OF WIND TURBINE BLADES USING GENETIC ALGORITHM AND PANEL METHOD INCLUDING BOUNDARY LAYER CORRECTIONS

Felipe José Vinaud, felipevinaud@gmail.com[1]
João Carlos Menezes, menezes@ita.br[2]
[1,2] ITA - Instituto Técnológico de Aeronáutica, Divisão de Engenharia Mecânica-Aeronáutica, CTA-ITA-IEM, Pça Mal. Eduardo Gomes n^o 50, 12228-900, São José dos Campos, SP, Brazil

Abstract. *The demand for electric energy has increased dramatically in the last years while the environmental effects and the sustainable use of energy are a reality that must be taken into account in the buildup of the energetic matrix of a country. As a consequence, the need for reliable and efficient means for generating electricity has brought up the necessity of developing optimization methods in the design of many machines, including wind turbines. This work presents the methodology for a genetic algorithm optimization of the cross section of wind turbine blades aiming at the maximum power coefficient (CP). Thus, the objective of the genetic algorithm is the minimization of the drag/lift ratio of a blade section. The PARSEC methodology was used to obtain a feasible geometry for the solution of the aerodynamic problem with only a few parameters. The panel method including boundary layer corrections with the Thwaite, Michel and Head methods are used to take into account viscous effects of laminar, transition and turbulent stages, respectively, in the solution of the flow field around the blade section. The results will allow for the choice of an approximate optimum geometry for the solution of a more complex CFD model in the future.*

Keywords: *wind turbine, genetic algorithm, panel method*

1. INTRODUCTION

In recent years it has been observed an increase in the demand for electrical power. Thus, a more efficient generation of power is to be assessed to optimize the operation of horizontal axis wind turbines (HAWT) and increase the extraction of energy from the wind. This work was proposed as a preliminary study of the running conditions of rotor blade geometry from an aerodynamic standpoint. For such, this article presents a simple study of the blade element theory used for determining the blade geometry taking into account phenomenon such as wake rotation. For attaining the drag to lift ratio, a linear vortex panel method is used to determine the lift coefficient. Thwaite's and Head's methods are used to determine the airfoil skin friction coefficient. The optimization procedure being implemented uses a parameterization scheme called PARSEC for 2D airfoil geometries based on useful geometric features such as leading edge radius and trailing edge cusp angle. This allows for the genetic algorithm code to choose geometry parameters that are more likely to give the maximum power coefficient (CP) for the respective blade element.

2. AERODYNAMICS OF WIND TURBINES

2.1 Momentum Theory

A wind turbine rotor consists of airfoils that generate lift through the pressure difference across the airfoil. In momentum theory, the flow field around a wind turbine rotor, is determined using the conservation of linear and angular momentum. This flow field is characterized by axial and angular induction factors that are a function of the rotor power extraction and thrust. According to Manwell *et al.* (2002), the geometry of the rotor and the lift and drag characteristics of the rotor airfoils can be used to determine either the rotor shape or rotor performance. The axial and angular induction factors are defined as:

$$a = \frac{U_1 - U_2}{U_1} \tag{1}$$

$$a' = \frac{\omega}{2\Omega} \tag{2}$$

where U_1 is the free stream velocity, $U2$ is the velocity at the rotor disc, ω is the angular velocity imparted to the flow stream and Ω is the velocity of the wind turbine rotor (see Fig. 1).

The forces on a wind turbine blade are derived considering the conservation of momentum. With the annular control volume shown in Fig. 1, the axial and angular induction factors are assumed to be functions of the radius r. From the conservation of linear momentum of the control volume of radius r and thickness dr the equation of the differential

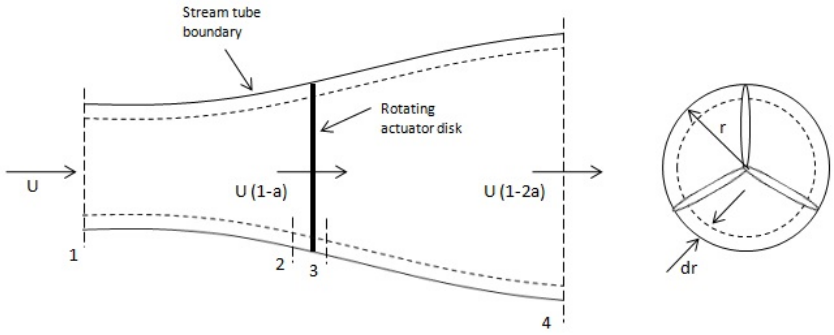

Figure 1. Geometry of rotor analysis; U, velocity of undisturbed air; a, induction factor; r, radius.

contribution to the thrust is:

$$dT = \rho U^2 4a\left(1-a\right)\pi r dr \tag{3}$$

From the conservation of angular momentum, the differential torque Q, imparted to the blades (equally and oppositely to the air) is:

$$dQ = 4a'\left(1-a\right)\rho U \pi r^3 \Omega dr \tag{4}$$

2.2 Blade Element Theory

The forces on the blades can be expressed as a function of lift and drag coefficients and the angle of attack. As shown in Fig. 2, the blade is assumed to be divided into N elements. Furthermore, it is assumed that there is no aerodynamic interaction between the elements and that the forces on the blades are determined solely by the lift and drag characteristics of the airfoil shape of the blades.

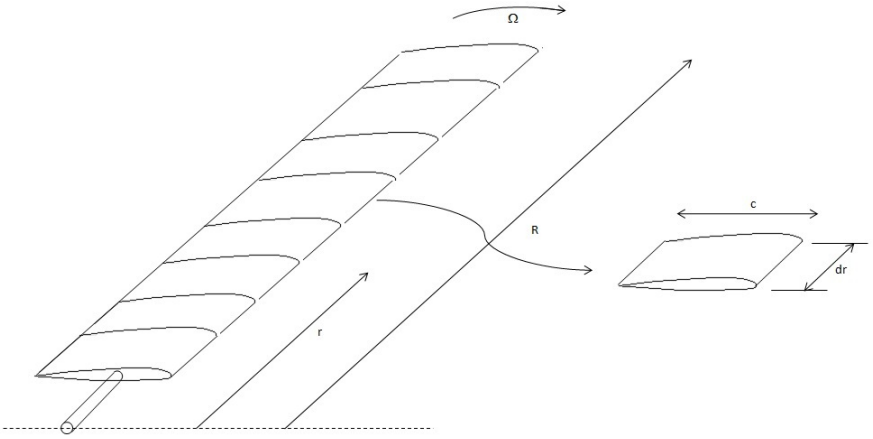

Figure 2. Schematic of blade elements: c, airfoil chord length; dr, radial length of element; R, rotor radius; Ω, angular velocity of rotor.

The lift and drag forces of a blade section are perpendicular and parallel, respectively, to an effective, or relative wind. The relative wind is the sum of the wind velocity at the rotor, $U(1-a)$, and the wind velocity due to rotation of the blade. This rotational component is the vector sum of the blade section velocity, Ωr, and the induced angular velocity at the blades from conservation of angular momentum, $\omega r/2$, or

$$\Omega r + \left(\omega/2\right) r = \Omega r + \Omega a' r = \Omega r\left(1+a'\right) \tag{5}$$

The the relationships of the various forces, angles and velocities at the blade, looking down from the blade tip, is shown in Fig. 3. Here, dF_L is the incremental lift force, dF_D is the incremental drag force, dF_N is the incremental force normal to the plane of rotation (contributing to thrust), and dF_T is the incremental force tangential to the circle swept by the rotor (force creating useful torque).

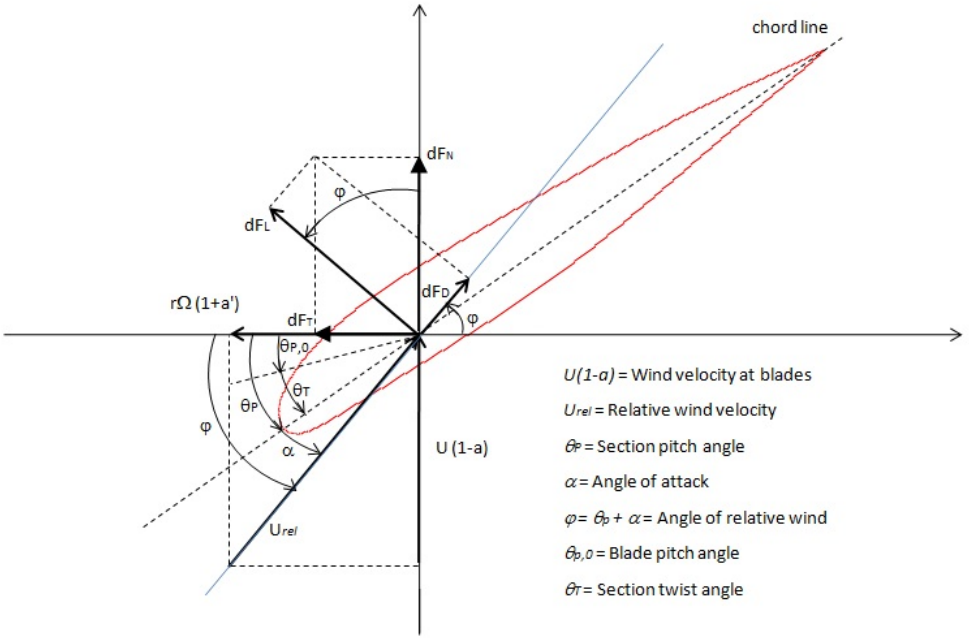

Figure 3. Blade geometry for analysis of a HAWT.

The differential torque due to the tangential force operating at a distance r from the center is given by

$$dQ = B\frac{1}{2}\rho U_{rel}^2 \left(C_l \sin\varphi - C_d \cos\varphi\right) c r dr \tag{6}$$

where B is the number of blades, C_l and C_d are the blade section lift and drag coefficients, c is the chord length of the section and r is the radial position of the blade section. Note that the effect of drag is to decrease torque and hence power, but to increase thrust loading.

2.3 Generalized Rotor Design Procedure

The procedure for determining the rotor design for specific conditions begins with the choice of various rotor parameters and the choice of an airfoil. The final blade shape and performance are determined iteratively. The steps in determining the blade design follow:

Determine basic rotor parameters

1. Begin deciding the power, P, and the wind speed, U. Include the effect of a probable C_p and efficiencies η of various components. The radius R of the rotor may be estimated from:

$$P = C_p \eta 1/2 \rho \pi R^2 U^3 \tag{7}$$

2. For electric power generation choose a tip speed ratio between 4 and 10. The higher speed machines use less material in the blades and have smaller gearboxes, but require more sophisticated airfoils. Usually for $\lambda > 4$ the number of blades B must be 3.

3. Select an airfoil. If $\lambda > 3$ a more aerodynamic shape must be used.

Define the blade shape

4. From the airfoil curves $C_{l,design}$ vs. $\alpha_{l,design}$ and $C_{d,design}$ vs. $\alpha_{l,design}$ chose the design aerodynamic conditions such that $C_{d,design}/C_{l,design}$ is at a minimum for each blade section

5. Divide the blade into N elements (usually 10-20). Use the following relations to estimate the shape of the *i*th blade with a midpoint of radius r_i:
local tip speed ratio

$$\lambda_{r,i} = \lambda(r_i/R) \tag{8}$$

local angle of relative wind

$$\varphi_i = tan^{-1}\left(\frac{2}{3\lambda_{r,i}}\right) \tag{9}$$

element chord length

$$c_i = \frac{8\pi r_i}{BC_{l,i}}\left(1-\cos\varphi_i\right) \tag{10}$$

element twist angle

$$\theta_{T,i} = \theta p, i - \theta p, 0 \tag{11}$$

also:

$$\varphi_i = \theta_{p,i} + \alpha_{design,i} \tag{12}$$

6. Using the optimum blade shape as a guide, select a blade shape that promises to be a good approximation. For ease of fabrication, linear variations of chord, thickness and twist might be chosen.

Calculate rotor performance and modify blade design

7. As outlined above the calculation of the rotor performance follows an iterative procedure to find the axial and angular induction factors. Initial guesses are needed and the values from an adjacent blade section or values from the previous blade iteration may be used. From the starting optimum blade design:

$$\varphi_{i,1} = tan^{-1}\left(\frac{2}{3\lambda_{r,i}}\right) \tag{13}$$

$$a_i, 1 = \frac{1}{\left[1+\frac{4sin^2(\varphi i,1)}{\sigma_{i,design}C_{l,design}\cos\varphi_{i,1}}\right]} \tag{14}$$

where σ is the local solidity or the ratio of the element area by the swept area defined as $\sigma = Bc/2\pi r_i$. The angular induction factor for the i*th* iteration is:

$$a'_{i,1} = \frac{1-3a_{i,1}}{(4a_{i,1})-1} \tag{15}$$

Having guesses for $a_{i,1}$ and $a'_{i,1}$, start the iterative solution procedure for the j*th* iteration. For the first iteration $j = 1$. Calculate the angle of the relative wind:

$$\tan\varphi_{i,j} = \frac{U\left(1-a_{i,j}\right)}{\Omega r\left(1+a'_{i,j}\right)} = \frac{1-a_{i,j}}{\left(1+a'_{i,j}\right)\lambda_{r,i}} \tag{16}$$

Determine $C_{l,i,j}$ and $C_{d,i,j}$ from the airfoil lift and drag data using:

$$\alpha_{i,j} = \varphi i, j - \theta_{p,i} \tag{17}$$

Calculate the local thrust coefficient

$$C_{T_r,i,j} = \frac{\sigma_i\left(1-a_{i,j}\right)^2\left(C_{l,i,j}\cos\varphi_{i,j} + C_{d,i,j}\sin\varphi_{i,j}\right)}{sin^2\varphi_{i,j}} \tag{18}$$

Update a and a' for the next iteration. If $C_{T_r,i,j} < 0.96$:

$$a_{i,j+1} = \frac{1}{\left[1+\frac{4sin^2\varphi_{i,j}}{\sigma_i C_{l,i,j}cos\varphi_{i,j}}\right]} \tag{19}$$

If $C_{T_r,i,j} > 0.96$:

$$a_{i,j} = 0.143 + \sqrt{0.0203 - 0.6427\left(0.889 - C_{T_r,i,j}\right)} \tag{20}$$

$$a'_{i,j+1} = \left[\frac{4cos\varphi_{i,j}}{\sigma C_{l,i,j}} - 1\right]^{-1} \tag{21}$$

If the newest induction factors are within an acceptable tolerance of the previous guesses, then the other performance parameters can be calculated. If not, then the procedure starts again at Equation 16.

8. Having solved the equations for the performance at each blade element, the power coefficient is determined using:

$$C_P = \frac{8}{\lambda N} \sum_{i=k}^{N} sin^2\varphi_i \left(cos\varphi_i - \lambda_{r,i} sin\varphi_i\right) \left(sin\varphi_i + \lambda_{r,i} cos\varphi_i\right) \left[1 - \left(\frac{C_d}{C_l}\right) cot\varphi_i\right] \lambda_{r,i}^2 \tag{22}$$

The total wind turbine thrust and torque is obtained by summing the results of the blade elements along the radial direction:

$$T = \sum_{i=k}^{N} \Delta T \tag{23}$$

$$Q = \sum_{i=k}^{N} \Delta Q \tag{24}$$

9. Modify the design if necessary and repeat steps 7-9 in order to find the best design for the rotor, given the limitations of fabrication.

3. AIRFOIL PARAMETERIZATION

In order to perform the optimization of the airfoil shape, such that the C_d/C_l ratio is minimized, a wide range of airfoil shapes, both known and unknown, must be analyzed. This can be done by means of a meta-model in which the C_d/C_l values of many airfoils are stored in a database and the optimization routine carries out the investigation of shapes from this database in order to search the best airfoil for the task. This methodology is presented by Menezes and Donadon (2009) and, usually, shapes are defined according to NACA series 4 and 5 geometries as in Ladson *et al.* (1996). Another approach is to parameterize the airfoil geometry according to desirable aerodynamic features. According to Mori *et al.* (2006) the changes implemented in the airfoil during a optimization procedure must be specified through geometric parameters instead of coordinates. These parameters can be used to define changes to the camber or the upper and lower skins of an airfoil profile.

In this paper, the methodology known as PARSEC by Sobieczky (1998) is implemented in order to apply changes to desirable features of the airfoil profile. Here, the airfoil is divided into a symmetric part and a camber line which are presented in the following polynomials:

$$t = a_1\sqrt{x} + a_2 x + a_3 x^2 + a_4 x^3 + a_5 x^4 \tag{25}$$

$$y_c = b_1 x + b_2 x^2 + b_3 x^3 + b_4 x^5 + b_5 x^6 \tag{26}$$

In the above equations, all the coefficients are expressed in terms of 11 basic parameters: leading edge radius, upper crest location, lower crest location and curvature, trailing edge coordinate at $X = 1$, thickness, direction and wedge angle. Figure 4 shows the scheme for the eleven parameters and a comparison between the NACA 23012 actual and PARSEC representations with an estimated error of 0.59%.

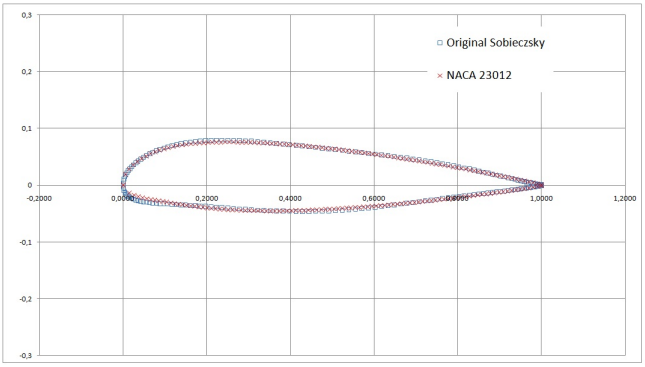

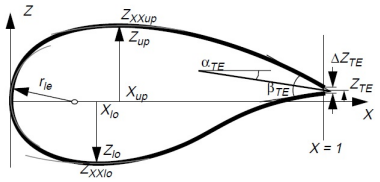

Figure 4. NACA23012 representation and PARSEC parameters

4. PANEL METHOD

An efficient way of determining the C_l and C_d values required in the iterative solution of the previous section is through the panel method. Many authors such as Anderson (1991) and Chow (1979) have implemented the potential flow

method. The method presented by Anderson (1991) is based on the discretization of the airfoil surface in panels over which singularities such as vortexes and sources are placed. The flow velocities are calculated at the center of each panel, where the contributions of the free stream flow and of each panel around the airfoil are summed up. The singularity strengths are calculated using a linear system of equations to satisfy the boundary conditions (normal component velocity component on each panel is 0). For the lifting flow case, another boundary condition is considered at the trailing edge where the tangential velocity at the panels on the upper and lower skins are made equal (one of the Kutta condition requirements). In the method presented by Anderson (1991) the Kutta condition applied at the trailing edge of the airfoil makes the linear system of equations overdetermined. In order to solve this linear system, one of the equations representing the flow boundary condition applied to one of the panels must be ignored. The choice of what equation to ignore is difficult since it may introduce some arbitrariness in the numerical solution.

This problem is overcome in the methodology by Houghton and Carpenter (2003) which mainly follows the original approach given by Hess and Smith (1967). Here, all the panels carry a source of strength σ_i and a vortex of strength γ. Since all the panels carry a vortex of equal strength the linear system of equations is easily solved adding one more term to the skin boundary condition and one more equation to satisfy the Kutta condition at the trailing edge making the system determined. Katz and Plotkin (2005) also provides a method for linear vortex strength variation along the individual panel surface. This method makes the velocity distribution over the airfoil more exact making it better for the use with boundary layer quantification methods.

4.1 Viscous Effects

Once the inviscid velocity and pressure profiles have been determined through the panel method, it is necessary to determine the velocity profile with viscous effects. With a new velocity profile the superficial friction coefficient can be obtained and thus the correct shear stress and friction drag coefficients are easily determined.

4.1.1 Thwaite's Method for Laminar Boundary Layers

According to Moran (1984), Thwaitet's method for laminar boundary-layer calculation is based on the integral momentum equation first derived by von Kármán and Pohlhausen for flat plates. The momentum integral equation is given by:

$$\frac{d\theta}{dx} + \frac{\theta}{V_e}(2+H)\frac{dV_e}{dx} = \frac{1}{2}c_f \quad \text{with} \quad H = \frac{\delta^*}{\theta} \tag{27}$$

where H is called the *shape factor* of the boundary-layer profile and relates the displacement thickness δ^* and the momentum thickness θ given by

$$\delta^* = \int_0^\infty \left[1 - \frac{u(x,y)}{V_e(x)}\right] dy \tag{28}$$

$$\theta = \int_0^\infty \frac{u}{Ve}\left(1 - \frac{u}{V_e}\right) dy \tag{29}$$

Thwaitet's method does not make any assumption on the form of the velocity profile and can be used in airfoils. Its basic aim is to suplement the momentum integral equation (27) with algebraic relations for the unknowns θ, H and c_f. Such relations will be simpler if in terms of dimensionless variables; thus θ and x are made dimensionless by forming Reynolds numbers:

$$Re_\theta = \frac{\rho V_e \theta}{\mu} \quad \text{and} \quad Re_x = \frac{\rho V_e x}{\mu} \tag{30}$$

A dimensionless and Reynolds independent skin friction parameter is introduced:

$$l = \frac{1}{2} Re_\theta c_f \tag{31}$$

Multiplying equation (27) through by Re_θ gives:

$$\frac{\rho V_e \theta}{\mu}\frac{d\theta}{dx} + \frac{\rho\theta^2}{\mu}(2+H)\frac{dV_e}{dx} = 1 \tag{32}$$

A dimensionless pressure-gradient parameter was also defined by Thwaite:

$$\lambda = \frac{\rho\theta^2}{\mu}\frac{dV_e}{dx} \tag{33}$$

Rewriting (32) using (33) yields to:

$$\frac{\rho V_e}{\mu}\frac{d\theta^2}{dx} = 2\left[l - (2+H)\,\lambda\right] \tag{34}$$

Thwaite found out that for exact solutions of boundary-layer equations in laminar flow l and H are functions only of λ. This function is approximated by:

$$2\left[l - (2+H)\,\lambda\right] \approx 0.45 - 6\lambda \tag{35}$$

When this function and the definiton of λ are substituted into Eq.(34) one obtains:

$$\frac{\rho V_e}{\mu}\frac{d\theta^2}{dx} = 0.45 - \frac{6\rho\theta^2}{\mu}\frac{dV_e}{dx} \tag{36}$$

Bringing the velocity gradient term to the left side and multiplying through by V_e^5 gives:

$$\frac{\rho}{\mu}\left(V_e^6\frac{d\theta^2}{dx} + \theta^2 6V_e^5\frac{dV_e}{dx}\right) = \frac{\rho}{\mu}\frac{d}{dx}\left(\theta^2 V_e^6\right) = 0.45V_e^5 \tag{37}$$

Thus, for any given $V_e(x)$ and initial value of θ, $\theta(x)$ can be determined by integration of a single first-order differential equation. According to Moran (1984), once θ is known, λ can be calculated from Eq.(33) and $l(\lambda)$ and $H(\lambda)$ can be calculated from correlation formulas given in Cebeci and Bradshaw (1977):

$$\begin{aligned}
l(\lambda) &= 0.22 + 1.57\lambda - 1.8\lambda^2 \quad \Rightarrow \quad 0 < \lambda < 0.1 && (38)\\
&= 0.22 + 1.402\lambda + \frac{0.018\lambda}{\lambda + 0.107} \quad \Rightarrow \quad -0.1 < \lambda < 0 && (39)\\
H(\lambda) &= 2.61 - 3.75\lambda + 5.24\lambda^2 \quad \Rightarrow \quad 0 < \lambda < 0.1 && (40)\\
&= 2.088 + \frac{0.0731}{\lambda + 0.14} \quad \Rightarrow \quad -0.1 < \lambda < 0 && (41)
\end{aligned}$$

Since for laminar boundary-layers it is needed a solution of a first order differential equation, the initial condition to be used for θ is: $\theta_0 = \sqrt{0.075\mu/(\rho\dot{V_0})}$.

4.1.2 Head's Method for Turbulent Boundary Layers

Head's method is based on the concept of an entrainment velocity. If $\delta(x)$ is the boundary-layer thickness, the volume rate of flow within the boundary layer at x is:

$$Q(x) = \int_0^{\delta(x)} u dy \tag{42}$$

The entrainment velocity E is the rate at which Q increses with x,

$$E = \frac{dQ}{dx} \tag{43}$$

Combinbing Eq.(42) with the definition of displacement thickness given in Eq.(28):

$$\delta^* = \delta - \frac{Q}{V_e} \tag{44}$$

Then

$$E = \frac{d}{dx}V_e\left(\delta - \delta^*\right) \tag{45}$$

can be writen as:

$$E = \frac{d}{dx}\left(V_e\theta H_1\right) \tag{46}$$

where

$$H_1 = \frac{\delta - \delta^*}{\theta} \tag{47}$$

Head ssumed that the dimensionless entrainment velocity E/V_e depends only on H_1 and that H_1, in turn, is a function of $H = \delta^*/\theta$. Cebeci and Bradshaw (1977) fit several sets of experimental data with the following formulas:

$$\frac{1}{V_e}\frac{d}{dx}\left(V_e \theta H_1\right) = 0.0306\left(H_1 - 3\right)^{-0.6169} \tag{48}$$

$$\begin{aligned} H_1 &= 3.3 + 0.8234\left(H - 1.1\right)^{1.287} \quad \Rightarrow H \leq 1.6 \\ &= 3.3 + 1.5501\left(H - 0.6778\right)^{-3.064} \quad \Rightarrow H > 1.6 \end{aligned} \tag{49}$$

Equations (27), (48) and (49) represent three equations among the four unknowns θ, H, H_1 and c_f. Head completes the set of Ludwieg-Tillman skin friction law:

$$c_f = 0.246 \times 10^{-0.678H} Re_\theta^{-0.268} \tag{50}$$

which was derived simply by fitting data available from various experimental studies with a formula of product form $f(H)g(Re_\theta)$. According to Moran (1984), it is accurate to $\pm 10\%$.

4.1.3 Transition From Laminar to Turbulent Flow

In the case of flow past an airfoil, the boundary-layer starts out as laminar at the stagnation point, with a finte thickness. Sooner or later, all boundary layers become unstable and any small disturbance initiates transition to turbulence. Among the more important factors that initiate instability are the pressure gradient imposed on the boundary layer by the inviscid flow and surface roughness. Transition is hastened, that is, the transition Reynolds number Re_x is lowered by both surface roughness and a positive value of dp/dx.

As stated in Moran (1984), for incompressible flows without heat transfer, Michel examined a variety of data and concluded that, for airfoil-type applications, transition should be expected when:

$$Re_\theta > 1.174\left(1 + \frac{22400}{Re_x}\right) Re_x^{0.46} \tag{51}$$

Although this formula accounts for pressure gradient effects, it does not take into account surface roughness effects. This is not useful for every application, but, being based on data taken from airfoils, it should be good for wing analysis.

Unfortunately the scatter of the data aboout Michelt's curve fit can amount to a large uncertainty as to the x at which transition occurs. Therefore, depending on the case, it will be necessary to bypass the use of Eq.(51) and impose transition at some point chosen with criteria. For example, it should not be expected the boundary layer to remain laminar much past the minimum pressure point. Also, a positive pressure gradient substantially decreases the stability of a laminar boundary layer, even at relatively low Reynolds numbers. Even more, a method like Thwaite's can give data on θ, H and c_f up to the start of transition, but H and c_f change so radically during transition that only the initial turbulent value of θ can be taken from calculations. So, it is suggested from literature that the value of H should be guessed since the shape factor of a turbulent boundary layer with a mild pressure gradient lies in the range of 1.3 to 1.4

4.1.4 Boundary Layer Separation

One characteristic of the velocity field in the vicinity of the separation point is that the nonslip condition applies both upstream and downstream of the separation point, so $u = 0$ at $y = 0$. However, at small values of y, $u > 0$ upstream of separation but $u < 0$ downstream. Thus the value at $y = 0$ of $\partial u/\partial y$ is positive upstream of separation and negative downstream, and hence zero at separation.

For example, in laminar flow (Thwaite's method), separation can be predicted to occur when $l(\lambda)$ vanishes, since l is defined in Eq.(31) to be proportional to the wall shear stress. According to the correlation formulas in Eqs.(38) to (41), this will happen when $\lambda = -0.0842$. A similar criterion is not possible in Head's method for turbulent boundary layers, however, since the skin friction given by the Ludwieg-Tillman skin-friction formula in Eq.(50) can never vanish. According to Moran (1984) one may predict turbulent separation by examining the development of the shape factor H, which is tipically about 2.4 at the start of separation.

5. GENETIC ALGORITHM OPTIMIZATION

To optimize the cross-section used in the analysis of Section 2. with the specific section wind profile, a genetic algorithm optimization will be performed. The genetic algorithm is an heuristic method based on the biological concepts

of natural selection and genetics. According to de Weck and Willcox (2004), in such scheme, for each interaction, the amount of changes termed as cross-overs, mutations and inheritance are set by the user and the choice of values to determine the PARSEC parameters is done randomly. After the current population is determined, each individual is assessed in terms of the aerodynamic analysis of Section 4. After that the more apt individuals are passed to the next generation of individual along with the most relevant features (genes).

6. PRELIMINAR PANEL METHOD RESULTS

Figure (5) below presents $Cl \times \alpha$ curve for an airfoil of type NACA 1410 obtained with the linear vortex and constant vortex panel methods without the use of boundary layer effects. The lift coefficient curve was obtained for a Reynolds number of 3000000 and compared with experimental results available in Abbot and Doenhoff (1959). Figure 6 curve shows the inviscid pressure distribution around the panel for a 2 degree angle of attack.

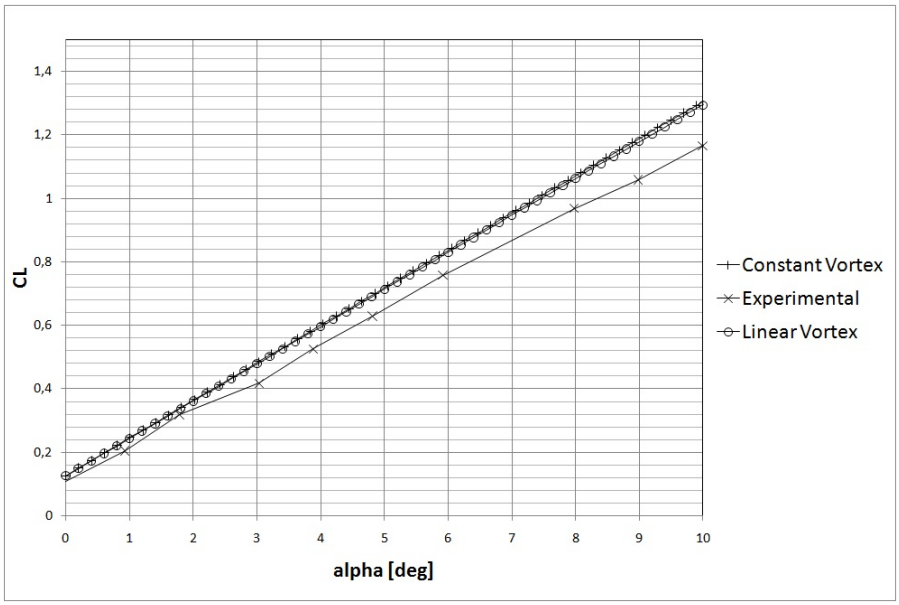

Figure 5. CL x α curve for airfoil NACA1410 at $Re = 3000000$

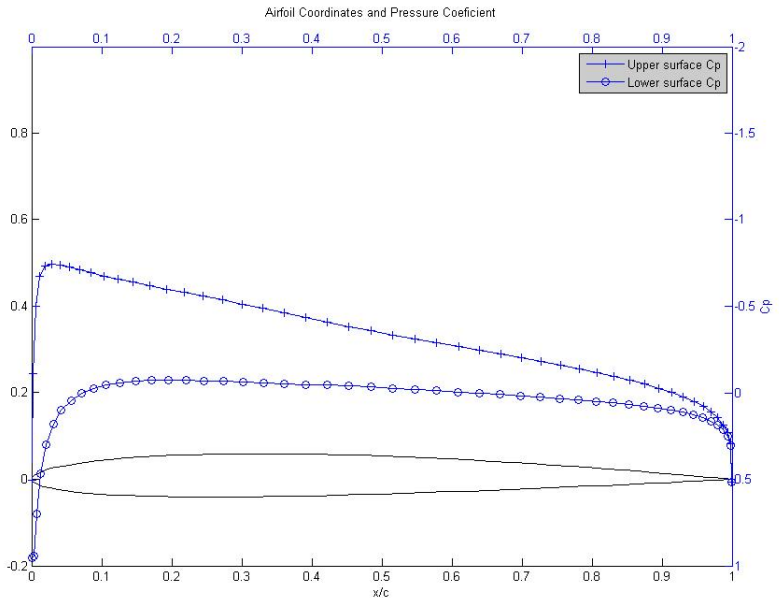

Figure 6. Pressure coefficient for airfoil NACA1410 at $Re = 3000000$ and $\alpha = 2$

7. CONCLUSIONS

This paper presented the guideline and preliminary results of a research aimed at optimizing a horizontal axis wind turbine from the aerodynamic standpoint. This optimization intends to enhance the power coefficient of a wind turbine blade including a phenomenon known as wake rotation. Effects like wing tip losses are not taken into account. The scheme to assess the blade power coefficient is termed blade element theory. In this theory, basic airfoil characteristics such as lift and drag coefficients are needed. For that, a panel analysis taking into account viscous effects must be carried out for the varying conditions of each element. The airfoil section chosen for each blade element is then chosen by a genetic algorithm optimization aimed at minimizing the C_d/C_l ratio of the airfoil. Steps aimed at determining the drag coefficient of a generic airfoil with low Reynolds numbers are currently being implemented and the genetic algorithm optimization to obtain the best possible blade profile will be implemented further.

8. REFERENCES

Abbot, I.H. and Doenhoff, A.E.V., 1959. *Theory of Wing Sections*. Dover Publications, Inc., New York, NY, USA.

Anderson, J.D., 1991. *Fundamentals of Aerodynamics*. McGraw-Hill, Inc., New York, USA.

Cebeci, T. and Bradshaw, P., 1977. *Momentum Transfer in Boundary Layers*. McGraw Hill/Hemisphere, Washington, D.C., USA.

Chow, C.Y., 1979. *An Introduction to Computational Fluid Dynamics*. John Wiley & Sons, Inc., New York, NY, USA.

de Weck, O. and Willcox, 2004. "Lecture notes from the MIT multidisciplinary system design optimization open course". MIT open course web site <http://ocw.mit.edu/OcwWeb/Aeronautics-and-Astronautics/16-888Spring-2004/LectureNotes/index.htm>.

Hess, J.L. and Smith, A.M.O., 1967. "Calculation of potential flow about arbitrary bodies". *Progress in Aerospace Sciences*, Vol. 8, pp. 1–138.

Houghton, E.L. and Carpenter, P.W., 2003. *Aerodynamics for Engineering Students*. Butterworth-Heinemann, Oxford, UK.

Katz, J. and Plotkin, A., 2005. *Low Speed aerodynamics*. Cambridge University Press, Cambridge, UK.

Ladson, C.L., Brooks, C.W., Hill, A.S. and Sproles, D.W., 1996. "Computer program to obtain ordinates for naca airfoils". NASA Technical Memorandum 4741.

Manwell, J.F., McGowan, J.G. and Rogers, A.L., 2002. *Wind Energy Explained - Theory, Design and Application*. John Wiley & Sons, LTD, West Sussex, England.

Menezes, J.C. and Donadon, M.V., 2009. "Optimum blade design of a 2 mw horizontal axis wind turbine". In *Proceedings of the 20th Brazilian Congress of Mechanical Engineering*. Rio de Janeiro, Brazil, Vol. 1.

Moran, J., 1984. *An Introduction to Theoretical and Computational Aerodynamics*. John Wiley & Sons, Inc., New York, NY, USA.

Mori, A.K., Fico, N.G.C.R. and Mattos, B.S., 2006. "Multi-point wing design of a transport aircraft using a genetic algorithm". In *44th AIAA Aerospace Sciences Meeting and Exhibit*. Reno, Nevada, USA, Vol. 1.

Sobieczky, H., 1998. "Parametric airfoils and wings". *Notes on Numerical Fluid Mechanics*, Vol. 68, pp. 71–88.

9. Responsibility notice

The authors are the only responsible for the printed material included in this paper